Desalination and Water Treatment
www.deswater.com
doi: 10.5004/dwt.2020.24993

178 (2020) 83–93
February

Characterization and application of activated carbon regenerated by the combination of sulfuric acid pretreatment and thermal regeneration

Wei Liu[a], Hong Yuan[a,b,*]

[a]*School of Chemistry and Chemical Engineering, North Minzu University, Yinchuan 750021, China, email: w.matics@gmail.com (W. Liu)*
[b]*State Key Laboratory of National Ethnic Affairs Commission Chemical Technology, North Minzu University, Yinchuan 750021, China, Tel. 86-18295215518; emails: yuanhong@nun.edu.cn (H. Yuan)*

Received 20 April 2019; Accepted 30 September 2019

ABSTRACT

Spent powdered activated carbon (SPAC) with pigments and impurities was regenerated via sulfuric acid pretreatment combined with thermal regeneration. The main purpose of this study was to restore and improve the adsorption performance of SPAC by exploring the effects of different regeneration conditions on regeneration. The results showed that at a sulfuric acid concentration of 1 mol/L, a solid–liquid ratio of SPAC to sulfuric acid of 50 g/L, a regeneration temperature of 500°C, and a regeneration time of 150 min, SPAC achieved the best regeneration effect. The iodine value and specific surface area (iodine value of 1,037 mg/g and Brunauer–Emmett–Teller (BET) surface area of 1,314 m^2/g) of the samples obtained under the optimal regeneration conditions were higher than those of virgin PAC (iodine value of 872 mg/g and BET surface area of 1,013 m^2/g). The regenerated samples were characterized by thermogravimetry, BET, scanning electron microscopy and Raman spectroscopy. Also, the Langmuir adsorption isotherm model showed better correlation for the adsorption of methylene blue (MB) on SA(1/50)S/500/150, indicating that monolayer adsorption occurs on the surface of activated carbon during adsorption. The kinetic experiments revealed that the mechanism of MB adsorption on SA(1/50)S/500/150 followed a pseudo second-order model.

Keywords: Spent powdered activated carbon; Sulfuric acid pretreatment; Thermal regeneration; Characterization; Methylene blue; Adsorption

1. Introduction

Due to its large specific surface area, developed pore structure, outstanding adsorption capacity, and stable catalyzing characteristics, activated carbon (AC) have been widely used in water treatment, gas separation, electrode materials preparation, industrial catalysis, and many other fields [1–4]. According to the differences in the appearance and shape of AC, it can be divided into powdered AC (PAC), granulated AC (GAC), amorphous granulated AC, cylindrical AC and many other shapes and forms. Among these, PAC has a faster adsorption rate and stronger decolorizing and deodorizing capabilities and has been extensively applied in the decolorization process of medicines [5], syrups [6] and dye wastewater [7]. However, the accumulation of adsorbates in the porous structure of AC gradually weakens its adsorption capacity. Once the adsorption capacity is saturated, AC is usually burned or landfilled, resulting in a waste of resources and environmental pollution. Regeneration treatment can restore the adsorption capacity of AC so that the regenerated activated carbon can be reused for multiple adsorption applications.

Thus far, a series of different regeneration methods have been utilized, such as thermal, chemical regeneration, electrochemical treatment, microwave regeneration, biological methods and others [8–12]. Among these regeneration

* Corresponding author.

methods, microwave regeneration has received increasing attention owing to its short regeneration time and its unique reverse heating mechanism, which is different from conventional heating. Contrary to conventional heating, Kostas et al. [13] pointed out that microwave heating involves the transfer of heat from within the materials to the surface, and the existence of a temperature gradient from the inside to outside is more conducive to the desorption of adsorbents. Also, Oliver [14] reported that the microwave heating effect is almost instantaneous, and there is no need to wait for the heating process, thus shortening the time of heating. However, the not-yet clarified mechanism of regeneration and safety of the regeneration device have restricted the actual application of this method. Electrochemical regeneration is feasible and potential new technology. Bain et al. [15] used anionic charged AC to adsorb cationic arsenic in aqueous solution. When the potential polarity was adjusted to be cathodic, the AC was completely regenerated. However, the slow development of this technology has hindered its application in industrial production [16,17]. Biological regeneration has the advantages of low cost and a simple regeneration process; however, biological pollution caused by microbial overgrowth seriously affects the regeneration results [18].

Although thermal regeneration requires high-energy consumption, thermal regeneration is still the most widely used regeneration method in industrial applications [19]. Thermal regeneration has a wide range of applications and can be applied to treat spent AC adsorbed with different organic substances, such as 1,2-dichloroethane [20], phenol [21], methyl ethyl ketone [22], benzene and toluene [23]. Also, this method has a high regeneration efficiency and can obtain a better regeneration effect. Berenguer et al. [21] compared the effects of chemical regeneration, thermal regeneration, and electrochemical regeneration on phenol-saturated AC. The results demonstrated that the regeneration efficiency of thermal regeneration increased with an increase in temperature, and the highest regeneration efficiency was 86% at 750°C. The highest efficiency of electrochemical regeneration was 85%, and chemical regeneration had the lowest regeneration efficiency of 65%. Okwadha et al. [24] studied the effect of temperature on the regeneration of mercury-adsorbed AC. At a regeneration temperature of 538°C, the removal rate of mercury reached 83%, and the specific surface area of PAC increased by 22%. The removal rate of mercury increased to 92% when the temperature increased to 649°C; however, the specific surface area of PAC decreased by 25%. Carratalá-Abril et al. [23] thermally regenerated AC with saturated adsorption of benzene and toluene in an oxygen atmosphere and analyzed the effect of adsorbent porosity on regeneration. The results showed that the activated carbons saturated with benzene could be regenerated at low temperatures (250°C–300°C), and good regeneration effects were observed after several cycles. The main reason for this was that these ACs possess a large mesopore volume and wide pore size distribution, which is conducive to the desorption and decomposition of adsorbates. Conversely, activated carbons saturated with toluene require higher temperatures (300°C–350°C) and show a lower regeneration efficiency. This can be attributed to their narrow pores. Román et al. [25] used steam as an activator to thermally regenerate AC saturated with p-nitrophenol (PNP). The effect of thermal regeneration was evaluated by comparing the adsorption capacities of regenerated and virgin activated carbon for N_2 and PNP. The results revealed that after thermal regeneration, the regeneration efficiency of N_2 adsorption reached 94%, and the regeneration efficiency of PNP adsorption was higher than 100%.

Chemical regeneration has the advantages of the investment of less equipment and a simple process; however, the regeneration efficiency is low. It often requires combination with the thermal regeneration method. Nahm et al. [26] compared three different regeneration methods, thermal regeneration, acid washing regeneration of a $C_2H_2O_4$ solution, and a two-step combined regeneration that involved thermal treatment after oxalic acid solution washing, and the results indicated that the combined chemical and thermal regeneration method was more effective than the separate thermal and chemical regeneration methods. The specific surface area of AC was obtained via two-step thermal treatment after oxalic acid solution washing is 852 m^2/g, whereas the specific surface areas of samples obtained via single oxalic acid solution washing and thermal regeneration were 83 and 771 m^2/g, respectively. Commonly used chemical regeneration solvents include hydrochloric acid [27], oxalic acid [26], sulfuric acid [28] and sodium hydroxide [29]. Among these regenerated solvents, sulfuric acid has attracted more attention because of its ideal regeneration effect. The use of sulfuric acid as an activator can weaken the physical interactions between organic compounds and activated carbon, reducing the reaction temperature; however, sulfuric acid in activated carbon particles can restrict the carbonization of organic compounds in the pores and prevent carbides from blocking the pores; additionally, the gases formed by sulfuric acid dehydration and thermal decomposition diffuse from the inside to the outside of the particles, resulting in many pores [30]. Zhou et al. [28] explored the effect of the thermal regeneration temperature on the adsorption performance of spent AC treated with or without sulfuric acid. The results showed that the adsorption capacity and pore structure of AC were better restored via the thermal regeneration process pretreated with sulfuric acid, and the highest iodine adsorption value of 1,294.69 mg/g was obtained at 600°C, which was close to the 1,306.67 mg/g of virgin AC. However, the regeneration temperature is not the only important factor that affects the regeneration effect of spent AC. Many other factors, such as the regeneration time, concentration of the chemical solvent, and the ratio of AC to chemical solvent, also play a very important role in the regeneration process. Systematic studies of the factors affecting the regeneration effect in the regeneration process can restore the adsorption performance of AC to the greatest extent, which is conducive to achieving the best regeneration effect; however, relevant literature is very scarce.

The main purpose of this work is to compare the regeneration effects of thermal regeneration with those of sulfuric acid pretreatment combined with thermal regeneration on spent powdered activated carbon (SPAC) used in decolorization in the pharmaceutical industry, to explore the optimal regeneration conditions and evaluate the adsorption performance of activated carbon obtained under the optimal regeneration conditions. In this study, we first adopted sulfuric acid pretreatment and then used the thermal regeneration

method to treat spent AC. The effects of the regeneration temperature, sulfuric acid concentration, solid–liquid ratio of spent AC to sulfuric acid, and regeneration time on the regeneration efficiency were studied. The adsorption equilibrium and kinetic behavior of methylene blue (MB) on AC were obtained under optimal regeneration conditions.

2. Experimental

2.1. Materials

SPAC and virgin PAC were provided by Ningxia Qiyuan Pharmaceutical Co. Ltd., China. Iodine, MB, and sulfuric acid are all analytical reagents.

2.2. Regeneration experiment

2.2.1. Thermal regeneration

The screened SPAC and virgin PAC with particle sizes of less than 74 μm were dried for 24 h at 105°C. The dried SPAC was heated to a target temperature (300°C–700°C) at a heating rate of 3°C/min under a vacuum atmosphere and maintained at this temperature for 30 min (sample notation: *S*/*T*/*t*, where *S* stands for SPAC, *T* represents the regeneration temperature, and *t* represents the regeneration time).

2.2.2. Thermal regeneration after sulfuric acid pretreatment

SPAC was mixed with sulfuric acid solutions (1, 2, and 3 mol/L) using varying solid–liquid ratios (50, 100 and 200 g/L) under magnetic stirring at room temperature for 1 h.

The mixture of SPAC and sulfuric acid solution was aged at room temperature for 24 h to ensure that the SPAC was fully impregnated. The pretreated SPAC was filtered, dried at 105°C for 12 h, and heated to a final temperature (300°C–700°C) for 30–210 min (sample notation: SA(*c*/*r*) *S*/*T*/*t*, where SA is the abbreviation for sulfuric acid, *c* represents the concentration of sulfuric acid, *r* represents the solid–liquid ratio of SPAC to sulfuric acid, and SA(*c*/*r*)*S* overall stands for SPAC pretreated with sulfuric acid).

2.2.3. Yield of regenerated activated carbon

The yield of regenerated activated carbon is an important factor in evaluating the regeneration efficiency and economic feasibility of the thermal regeneration process. Eq. (1) was used to calculate the regeneration yield.

$$\text{Yield}(\%) = \frac{M_1}{M_0} \times 100\% \tag{1}$$

where M_0 is the mass of sample before regeneration and M_1 is the remaining mass of sample after regeneration.

2.3. Characterization methods

The iodine and MB values for the regenerated samples were determined by standard testing methods of PR China (GB/T 12496.8-1999 and GB/T 12496.10-1999), respectively.

The SPAC and SA(1/50)S were characterized by thermogravimetric analysis using a simultaneous thermal analyzer (NETZSCH STA 449 F5). The samples were heated from 50°C to 900°C at a rate of 10°C/min. The analysis was conducted in a nitrogen atmosphere with a nitrogen flow rate of 50 mL/min.

The nitrogen adsorption–desorption isotherm at 77 K was measured by a specific surface area and porosity analyzer (Micromeritics ASAP 2020, Norcross, GA, USA). Before sample analysis, vacuum degassing was conducted at 300°C for 4 h. The following parameters were calculated based on nitrogen isotherm data: (a) the specific surface areas (S_{BET}) of the samples were calculated by the Brunauer–Emmett–Teller (BET) method [31], (b) the micropore volume (V_{mic}) was determined by the *t*-plot method [32], (c) the mesopore volume was calculated by the DFT method [33], (d) the single-point adsorption total pore volume of the pores (V_{total}) was obtained at a relative pressure of 0.99, the average pore width (D) was calculated by $4V_{total}/S_{BET}$, and (e) the pore size distribution was determined by the BJH equilibrium model.

The microstructures of the samples were examined by a tungsten filament scanning electron microscope (ZEISS EVO18, Neubeuern, BA, BRD) at an acceleration voltage of 15 KV.

The carbon, hydrogen, oxygen, and nitrogen contents of the samples were analyzed by an ICP-OES (Agilent 730 ICP-OES, Santa Clara, CA, USA).

Raman spectra were recorded on a spectrometer (Renishaw System 2000, Kane, IL, USA) at room temperature.

2.4. Adsorption experiments

In this experiment, AC was used to adsorb pigment organics. Therefore, the adsorption behavior of regenerated sample SA(1/50)S/500/150 on the adsorbate was studied using MB as the model compound.

2.4.1. Adsorption isotherm

MB adsorption experiments were performed by adding a 20 mL MB (800–1,200 mg/L) solution at different initial concentrations and 0.05 g of regenerated AC to a group of Erlenmeyer flasks (100 mL). The adsorption time was maintained for 5 h using a gas bath thermostatic oscillator, and the adsorption temperatures were 303, 318 and 333 K. The solution was centrifugally separated after oscillation equilibrium, and its absorbance was determined by a UV spectrophotometer at 665 nm after 100 times dilution.

The equilibrium adsorption capacity of MB (q_e) on AC was determined through the following equation:

$$q_e = \frac{(C_i - C_e)V}{M} \tag{2}$$

where C_i and C_e are the MB concentration at initial and at equilibrium, respectively (mg/L). V is the volume of MB solution (L) and M is the mass of the added activated carbon (g).

2.4.2. Adsorption kinetics

The process of the MB adsorption kinetics experiment was the same as that of the equilibrium adsorption experiment, except that the concentration of MB was controlled at 1,000 mg/L and the adsorption temperature was controlled

at 303 K. In the first 15 min of the adsorption experiment, an Erlenmeyer flask was taken out every 5 min to determine the absorbance of the supernatant. After 30 min of adsorption, the absorbance of the supernatant was determined every 30 min. The total adsorption time was 210 min.

The momentary adsorption capacity of MB (q_t) on AC was calculated according to the following equation:

$$q_t = \frac{(C_i - C_t)V}{M} \tag{3}$$

where C_i and C_t are the MB concentration at initial and at pre-determined time t, respectively (mg/L). V is the volume of MB solution (L) and M is the mass of the added activated carbon (g).

3. Results and discussion

3.1. Thermogravimetric analysis

The thermogravimetric (TG) and differential thermogravimetric (DTG) curves of the dried SPAC and SA(1/50)S heated from 50°C to 900°C are shown in Fig. 1. According to Fig. 1a, the pyrolysis process of SPAC can be divided into three stages. The first stage from 50°C to 150°C is related to the moisture loss of the material. In the second stage (150°C–500°C), the volatile organic compounds that were physically adsorbed on AC were removed. As shown from the DTG curve, there are two obvious weightlessness peaks present at this stage, which are both rapid weightlessness processes. In the third stage (500°C–900°C), the removal of compounds that were chemically adsorbed on AC and the cracking of surface functional groups occurred [34,35]. As shown in Fig. 1b, two weightlessness peaks in the DTG curve moved forward owing to H_2SO_4 pretreatment, and the former one moves more widely. The TG curve shows that the first stage of the pyrolysis process occurs at a lower temperature (50°C–100°C), and the second stage occurs at 100°C–450°C after sulfuric acid pretreatment. According to the literature [28], pretreatment with H_2SO_4 can weaken the physical interaction force between adsorbates and adsorbents, which results in desorption of adsorbates at a lower temperature. In addition, the TG curve shows that the relative residual mass of SA(1/50)S was higher than that of SPAC at the end of pyrolysis. This may be because, during the process of sulfuric acid pretreatment, some organic substances and impurities adsorbed on the surface of SPAC via weak physical action were removed in advance so that two samples with the same relative mass had different relative residual masses after pyrolysis.

3.2. Regeneration of ACs

3.2.1. Effect of regeneration temperature on the iodine value and yield of SPAC and SA(1/50)S

Fig. 2a shows the influence of sulfuric acid pretreatment on the adsorptive capacity of the regenerated samples. The regenerated samples pretreated by sulfuric acid had a higher iodine value than the samples without sulfuric acid pretreatment. This result indicated that appropriate sulfuric acid pretreatment could achieve a better regeneration effect. With an increase in temperature, the iodine value of the two regenerated samples showed a trend of increasing at first and then decreasing. The reason for this phenomenon may be the increase in temperature gradually restored the microporous structure of AC, and the surface oxygen functional groups were decomposed considerably. A further increase in temperature resulted in the collapse of the pore walls of AC and blocking of the pores. According to the literature, oxyacid pretreatment can increase the number of surface oxygen-containing groups on AC. These groups then preferentially adsorb water molecules from the aqueous solution to form water clusters, preventing the removal of organic compounds [36,37]. The maximum iodine values of S/500/30 and SA(1/50)S/500/30 were 857 and 862 mg/g, respectively, which had not yet been restored to the iodine value of virgin AC. The exploration of the optimal conditions for sulfuric acid pretreatment and the reasons for the different regeneration effects of different pretreatment conditions will be further explained in the next section.

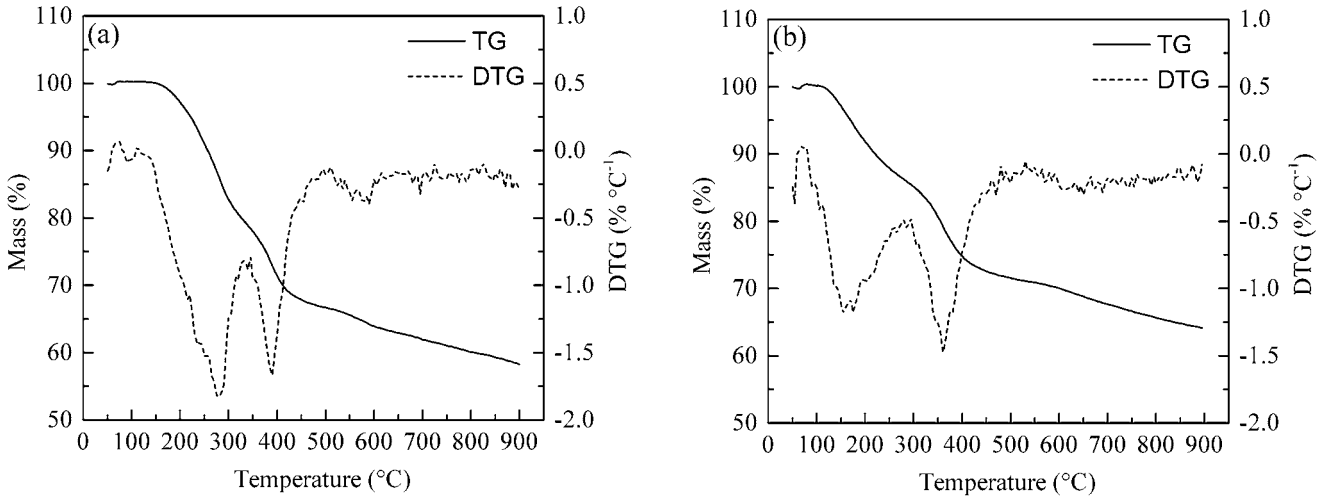

Fig. 1. Thermogravimetric and differential thermogravimetric curves of SPAC (a) and SA(1/50)S (b).

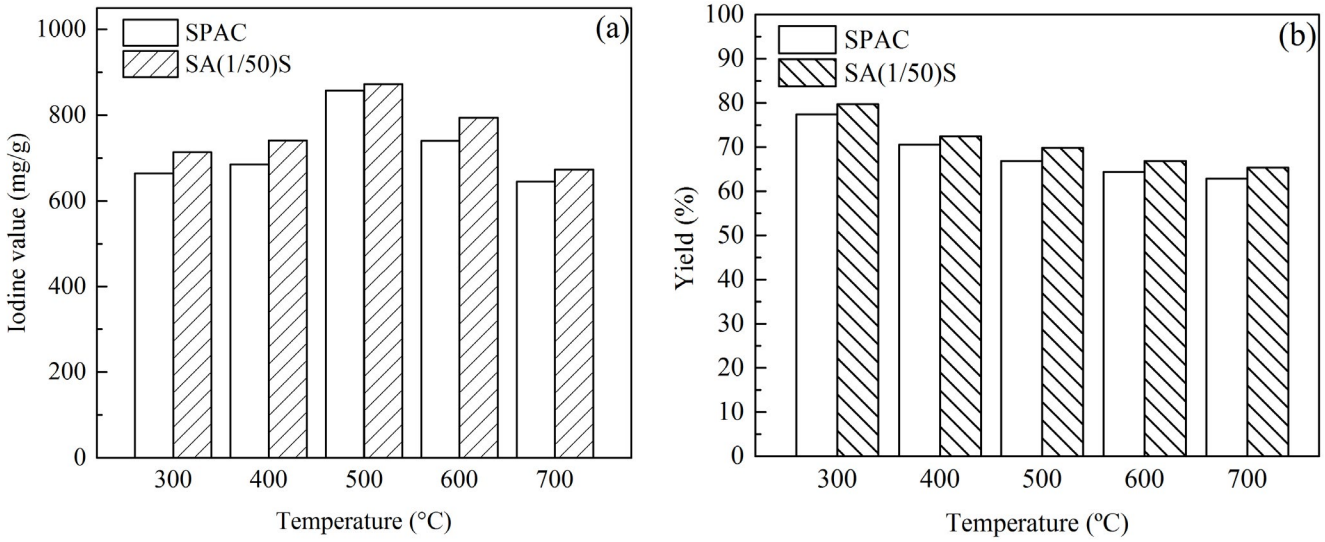

Fig. 2. (a) Iodine values of regenerated SPAC and SA(1/50)S at different temperatures (experimental conditions: sulfuric acid concentration of 1 mol/L, the solid–liquid ratio of AC to sulfuric acid of 50 g/L, and regeneration time of 30 min). (b) The yield of regenerated activated carbon with or without sulfuric acid pretreatment (experimental conditions: sulfuric acid concentration of 1 mol/L, the solid–liquid ratio of AC to sulfuric acid of 50 g/L, and regeneration time of 30 min).

The yield of regenerated activated carbon with and without sulfuric acid pretreatment was evaluated at different temperatures. As shown in Fig. 2b, the yield of regenerated sample decreases as the temperature increases and still exceeds 62% at 700°C, indicating that the regenerated AC offers good stability and economic feasibility. Additionally, the yield of regenerated activated carbon pretreated with sulfuric acid is higher than that of activated carbon untreated with sulfuric acid, which is consistent with the TG results.

3.2.2. Effect of sulfuric acid concentration, solid–liquid ratio and regeneration time on the iodine value of SPAC

The influence of different sulfuric acid concentrations, solid–liquid ratios, and regeneration times on the iodine value were evaluated by keeping the other influencing factors unchanged for the same experimental process: (a) at a solid–liquid ratio of 50 g/L and regeneration temperature of 500°C; (b) at a sulfuric acid concentration of 1 mol/L and a regeneration temperature of 500°C. The results are shown in Fig. 3. At a sulfuric acid concentration of 1 mol/L, a solid–liquid ratio of 50 g/L, and a regeneration time of 150 min, the regenerated samples achieved an iodine value of 1,037 mg/g, which was higher than that of virgin PAC. This may be because sulfuric acid acts as an activator under suitable regeneration conditions and reactivates the AC. Continued regeneration and activation processes can restore the original pores of AC while enabling AC to produce new pores, thus enhancing its adsorptive capacity.

Fig. 3a shows the influence of different sulfuric acid concentrations and regeneration times on the iodine value of the regenerated samples. As shown, with the same regeneration time, the iodine adsorption capacity of the regenerated samples decreased with an increase in sulfuric acid concentration, and the maximum iodine value achieved was 1 mol/L. This could be due to the change in the pore structure of AC along with the increase in sulfuric acid concentration; the severely damaged microporous structure of the regenerated samples was not conducive to the adsorption of iodine molecules. Fig. 3b shows the influence of different solid–liquid ratios and regeneration times on the iodine value of the regenerated samples. For the same time, the iodine value of the regenerated samples first decreased and then increased with a decrease in the ratio of material to liquid, and the maximum iodine value obtained was 50 g/L. This may be because the amount of sulfuric acid increased as the ratio of solid to liquid decreased. The formation of an active center with sulfuric acid as the activator damaged the microporous structure of the material to some extent, which led to a downward trend in the adsorptive capacity of AC [38]. At a certain sulfuric acid dosage, an active center was formed with an increased contact area between the activator and the material. This facilitated the formation of more micropores, resulting in an upward trend in the adsorptive capacity of AC [39].

Moreover, with a longer regeneration time, the iodine values of regenerated samples with different sulfuric acid concentrations and solid–liquid ratios presented a trend of initial increases followed by a decrease. The reason may be the gradually restored pore structure of SPAC along with the longer regeneration time, which caused the iodine value to increase. When the regeneration time exceeded 150 min, the micropores restored via regeneration and those produced by activation gradually turned into mesopores and macropores, resulting in a downward trend in the iodine values of the regenerated samples.

3.3. Surface area and pore structure

Fig. 4a shows the nitrogen adsorption–desorption isotherms of spent AC, fresh AC, and regenerated AC, which

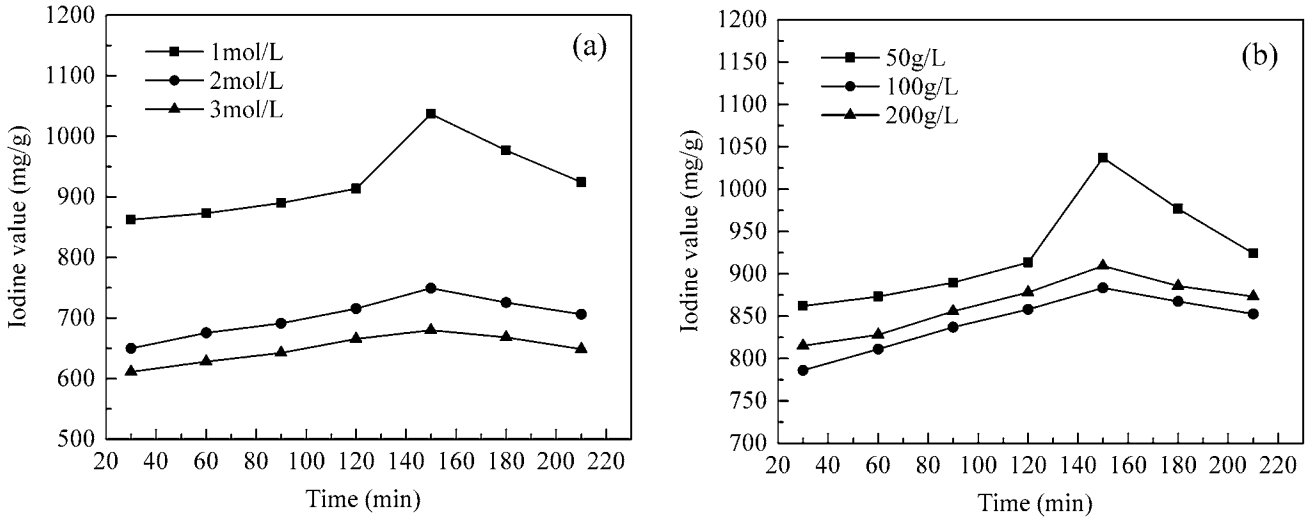

Fig. 3. Iodine value of regenerated SPAC at different sulfuric acid concentrations, solid–liquid ratios, and times (experimental conditions: (a) solid–liquid ratio of 50 g/L and regeneration temperature of 500°C and (b) sulfuric acid concentration of 1 mol/L and regeneration temperature of 500°C).

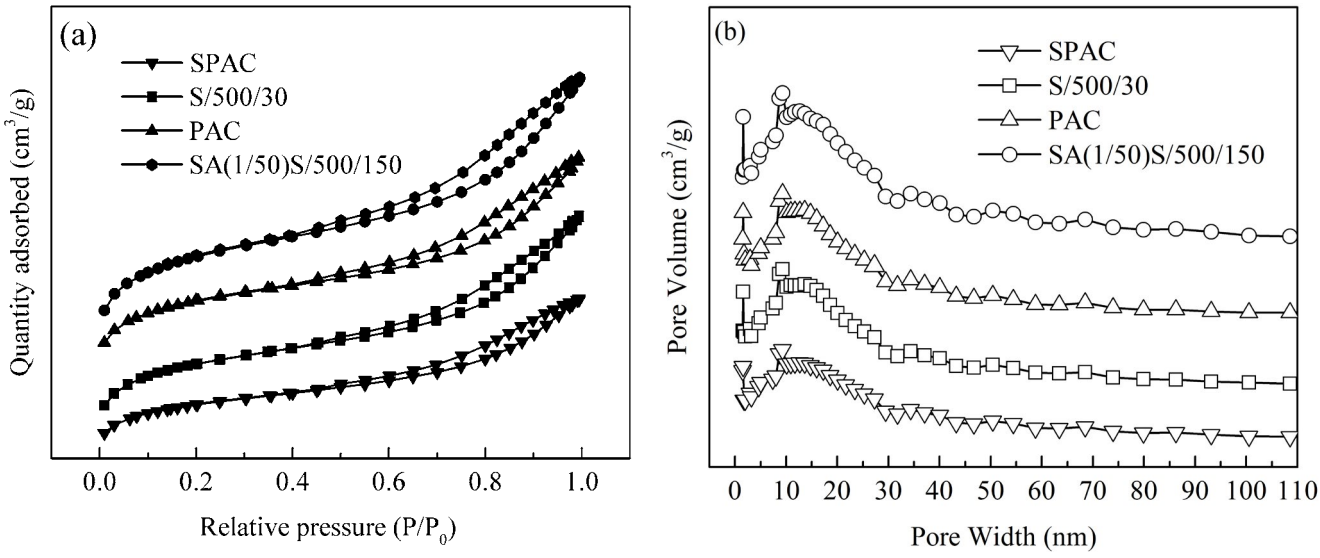

Fig. 4. N_2 adsorption–desorption isotherms and pore size distributions of various samples.

are all IV isotherms. When $P/P_0 < 0.4$, the adsorption isotherm overlapped the desorption isotherm, and monolayer adsorption occurred; when $P/P_0 > 0.4$, they were separated due to capillary condensation in the mesopores and macropores, and an H_4 type hysteresis loop appeared, which indicated that the samples contained a certain amount of slit sharp mesoporous generated from a flaky structure [40]. The higher nitrogen adsorption capacity of sample SA(50/1)S/500/150 compared with virgin AC under the same relative pressure suggested that sulfuric acid acts as an activator during the regeneration process so that new pores generate in the AC and thus improve its adsorption capacity, which is consistent with the iodine value measured. The nitrogen adsorption capacity of S/500/30 was lower than that of the virgin AC, which indicated that thermal regeneration could not restore the adsorption capacity of SPAC to its original state.

Fig. 4b shows the pore size distribution curves for the four samples. As shown, the pore sizes of AC are mainly distributed within 2–20 nm, indicating that the four kinds of AC samples have a large number of mesopores. Moreover, these four samples exhibit distinct pore size distributions in the range 0–2 nm, indicating that they contain large numbers of micropores.

Table 1 summarizes the specific surface areas and pore structure parameters of the different AC samples. As shown in this table, the specific surface area of S/500/30 was 950 m^2/g, which was restored to 93.8% of the virgin PAC (1,013 m^2/g). With the same regeneration temperature and regeneration

Table 1
Surface areas and porosity characteristics of PAC, SPAC and regenerated activated carbons

Samples	S_{BET} (m^2/g)	V_{micro} (cm^3/g)	V_{meso} (cm^3/g)	V_{tot} (cm^3/g)	I_2 value (mg/g)	D (nm)
PAC	1,013	0.182	0.863	1.065	872	4.2
SPAC	592	0.057	0.574	0.614	528	4.8
S/500/30	950	0.135	0.838	1.051	857	4.4
SA(1/50)S/500/30	999	0.177	0.832	1.060	862	4.3
S/500/150	822	0.109	0.726	0.903	779	4.5
SA(1/50)S/500/150	1,314	0.224	1.087	1.351	1,037	4.1

time, the specific surface area of the regenerated sample pretreated with sulfuric acid (SA(1/50)S/500/30) was 999 m^2/g, accounting for 98.6% of virgin PAC, indicating that sulfuric acid pretreatment had a better effect on the recovery of the specific surface area of spent AC. When the regeneration time was prolonged from 30 to 150 min, the specific surface area and pore volume of the regenerated sample (S/500/150) without sulfuric acid pretreatment decreased, whereas the specific surface area and pore volume of SA(1/50)S/500/150 considerably increased. The specific surface area of SA(1/50) S/500/150 grew to 1,314 m^2/g, the micropore volume and mesopore volume recovery rate were 123% and 125.9%, respectively, and the average pore diameter decreased from 4.2 to 4.1 nm, suggesting that the regeneration time, when extended appropriately, would assist in recovering the specific surface area and pore structure of the sulfuric acid-pretreated AC.

A comparison of specific surface areas of ACs is shown in Table 2. As indicated in Table 2, the specific surface areas of regenerated ACs with acid pretreatment were close to or exceeded those of virgin ACs, indicating that acid pretreatment of spent ACs during the thermal regeneration process improves the regeneration effect. Additionally, although the specific surface area of the regenerated activated carbon in this study is not the largest of those reported, its value shows the most significant increase among all fully regenerated activated carbons. This indicates that systematically exploring the factors affecting the regeneration effect is conducive to achieving better regeneration results.

3.4. Scanning electron microscopy

SEM images of the SPAC, S/500/30, and SA(1/50)S/500/150 samples are shown in Fig. 5. Fig. 5a clearly shows the surface characteristics of the spent AC in which a large number of impurities were attached on its surface and completely covered its structure in a membrane shape. This prevented the adsorbates from entering its inner pores and reduced its adsorption capacity. As shown in Fig. 5b, impurities that were adsorbed on the surface of AC were effectively removed via thermal regeneration, and its adsorption capacity was restored. Fig. 5c shows the morphologic characteristics of SA(1/50)S/500/150. Part of the surface covering impurities was removed, and with abundant pore channels on the surface of the sample and a clear structure, the adsorption capacity of AC was restored.

3.5. ICP-OES

The ICP-OES results for SPAC, S/500/30 and SA (1/50) S/500/150 are shown in Table 3. The C, H, O and N contents of SPAC are 52.34%, 16.09%, 5.93%, and 9.44%, respectively. Compared with SPAC, the carbon content increased while the nitrogen and hydrogen contents decreased in the two regenerated samples. This behavior was due to the decomposition of adsorbed organic compounds during regeneration. After thermal regeneration by sulfuric acid pretreatment, the nitrogen content in SPAC decreased from 9.44% to 5.52%, while that in S/500/30 was 5.78%. The results showed that the nitrogen-containing organic compounds adsorbed in AC could be removed more effectively by thermal regeneration after sulfuric acid pretreatment. The oxygen content in SA (1/50)S/500/150 was the highest, which may be due to oxidation of sulfuric acid during regeneration.

3.6. Raman spectra

Fig. 6 shows the Raman spectra of SPAC and the regenerated AC. As shown, the D peak owing to disorder and the

Table 2
Comparison of specific surface area of ACs

Adsorbent	Regeneration	Specific surface area (m^2/g)		Ref.
	solvents	Regenerated AC	Virgin AC	
GAC	–	615	971	[35]
PAC	–	1,726	2,825	[41]
PAC	$C_2H_2O_4$	852	823	[26]
PAC	H_2SO_4	1,839	2,112	[28]
PAC	H_2SO_4	1,314	1,013	This work

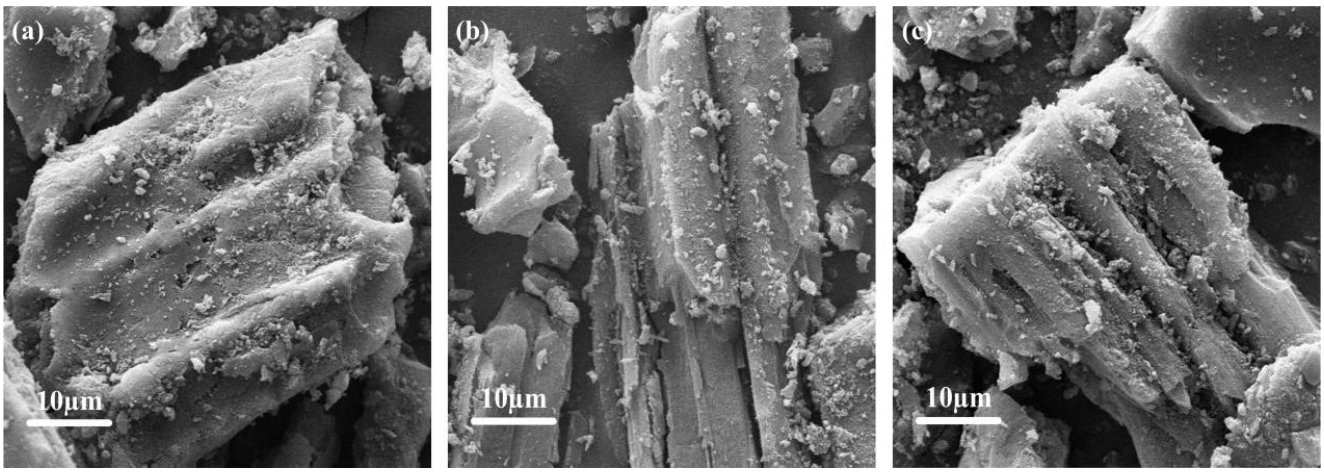

Fig. 5. SEM images of the (a) SPAC, (b) S/500/30 and (c) SA(1/50)S/500/150.

Table 3
ICP-OES of SPAC and regenerated samples

Sample	C (%)	H (%)	O (%)	N (%)
SPAC	52.34	16.09	5.93	9.44
S/500/30	56.38	14.77	3.43	5.78
SA(1/50)S/500/150	55.63	15.61	10.82	5.52

G peak owing to crystalline graphitization were located at 1,330 and 1,580 cm^{-1} [42], respectively. The intensity ratio R (I_D/I_G) between the D peak and the G peak reflects the degree of disorder and graphitization in carbon materials. A larger ratio represents a lower degree of graphitization and a higher degree of disorder for carbon materials [43,44].

Table 4 shows the intensity ratio between the D and G peaks of different AC samples. As shown in the table, compared with SPAC, thermal regeneration after sulfuric acid pretreatment enhanced the I_D/I_G value, while thermal regeneration without the sulfuric acid pretreatment decreased the I_D/I_G ratio. This indicated that the sulfuric acid pretreatment reduced the degree of graphitization and increased the degree of disorder for these carbon materials [45]. In addition, the increase in regeneration temperature enhanced the I_D/I_G ratio with or without sulfuric acid pretreatment. These results indicate that the increase in regeneration temperature can reduce the degree of graphitization and enhance the disorder degree of carbon materials [46].

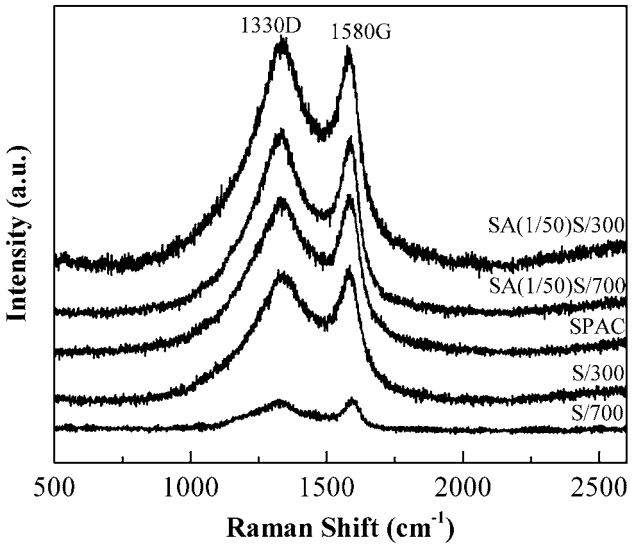

Fig. 6. Raman spectra of SPAC and the regenerated AC samples.

Table 4
Intensity ratio of the D and G bands (I_D/I_G) of SPAC and regenerated activated carbon samples

Sample	SPAC	S/300	S/700	SA(1/50)S/300	SA(1/50)S/700
R	1.009	0.954	0.966	1.041	1.104

3.7. Adsorption of MB

3.7.1. Adsorption isotherm

The equilibrium adsorption data of MB were fitted using Langmuir and Freundlich isotherm models, as shown in Eqs. (3) and (4):

$$q_e = \frac{q_m K_L C_e}{1 + K_L C_e} \tag{4}$$

$$q_e = K_F C_e^n \tag{5}$$

The q_m and K_L constants are the Langmuir constants, which indicates the maximum adsorption capacity of an adsorbent for MB (mg/g), and the Langmuir isotherm constant, which is related to the adsorption properties (L/mg), respectively. K_F and n are Freundlich constants that represent the adsorption amount and adsorption intensity of the sorbent, respectively.

Isothermal adsorption experiments were performed according to the experimental steps described in Section 2.4.1. The Langmuir and Freundlich equations were used to fit the isothermal adsorption data. The fitting results are shown in Figs. 7 and 8. Fitting parameters K_L, K_F and q_m are shown in Table 5. As indicated by the results, the Langmuir isothermal adsorption model has good fitting results for the adsorption of MB via regenerated AC because the correlation coefficient, R^2, at the three temperatures is above 0.999, indicating that mainly monolayer adsorption occurs in the system. As the system temperature increased from 303 to 333 K, there was an increase in equilibrium adsorption capacity from 357.14 to 384.62 mg/g, indicating that the increase in temperature is conducive to the adsorption reaction and that the adsorption process is endothermic. The reason may be that an increase in temperature decreases the viscosity of the system, increases the fluidity of the solution, and allows the MB molecules to gain more energy to interact with the adsorption sites on the surface of AC.

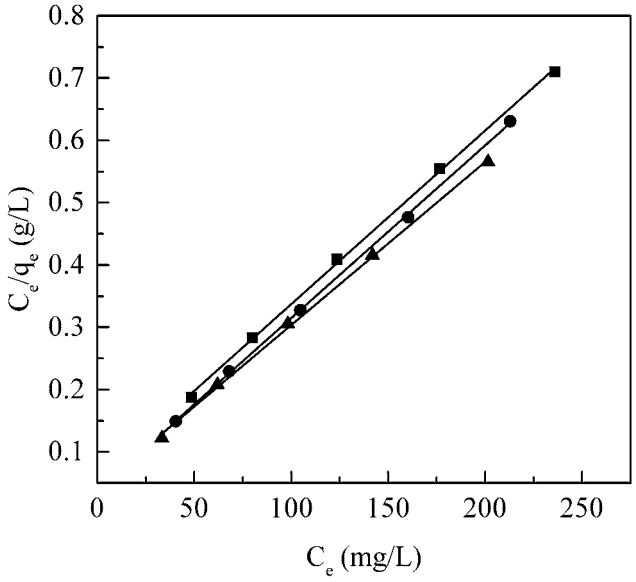

Fig. 7. Langmuir isotherms for MB adsorption onto SA(1/50) S/500/150 at different temperatures.

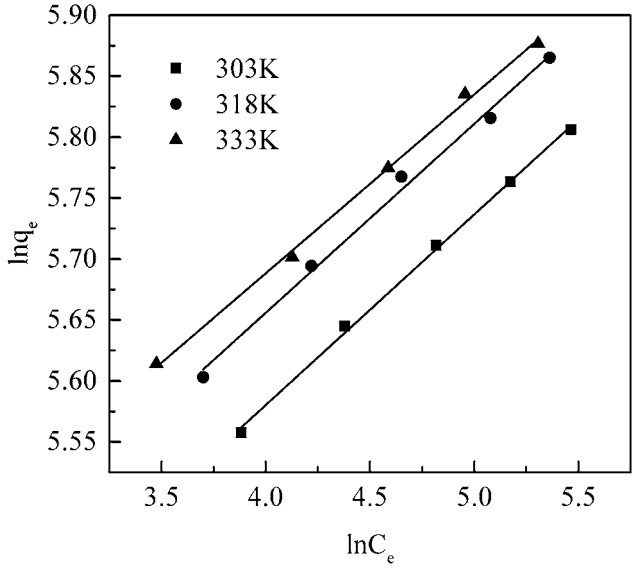

Fig. 8. Freundlich isotherms for MB adsorption onto SA(1/50) S/500/150 at different temperatures.

3.7.2. Adsorption kinetics

Pseudo first-order and pseudo second-order kinetic equations were applied to describe the kinetic characteristics of MB on the regenerated AC. The integrated linear form of the pseudo first-order and pseudo second-order kinetic equations can be expressed via Eqs. (5) and (6).

$$\log\left(q_e - q_t\right) = \log q_e - \frac{K_1 t}{2.303} \tag{6}$$

$$\frac{t}{q_t} = \frac{1}{K_2 q_e^2} + \frac{t}{q_e} \tag{7}$$

where K_1 (min^{-1}) and K_2 (g/mg min^{-1}) are the rate constants of the pseudo first-order and the pseudo second-order, respectively.

The adsorption kinetics experiment was conducted according to the experimental steps described in Section 2.4.2. The experimental data were fitted and analyzed by the pseudo first-order kinetic and the pseudo second-order kinetic equations. The fitting results are shown in Figs. 9 and 10. The rate constant, K, the estimated equilibrium uptake, $q_{e,\mathrm{cal}}$, and the correlation coefficient, R^2, are summarized in Table 6. As shown from the results, the correlation coefficient of the pseudo second-order kinetic model was above 0.999, and the equilibrium adsorption capacity, $q_{e,\mathrm{cal}}$, calculated from this model was similar to the equilibrium adsorption capacity, $q_{e,\mathrm{exp}}$, measured during the experiment. This indicates that the pseudo second-order kinetic equation can be well used to describe the kinetic behavior of AC adsorption of MB. Similar studies by Zhou et al. [28] on the removal of MB from aqueous solution showed a maximum adsorption capacity of 429 mg/g, calculated using a pseudo second-order model, which was similar to the equilibrium adsorption capacity of 426 mg/g measured during the experiment. The similar adsorption capacities obtained in this study suggest the use of a pseudo second-order kinetic model to describe the kinetic behavior of AC adsorption of MB.

Table 5
Isotherm parameters for removal of MB by SA(1/50)S/500/150 at different temperatures

Temperature (K)	Langmuir			Freundlich		
	K_L	q_m	R^2	K_F	n_F	R^2
333	0.064	384.62	0.999	164.22	6.81	0.998
318	0.057	370.37	0.999	153.90	6.46	0.995
303	0.048	357.14	0.999	141.85	6.39	0.998

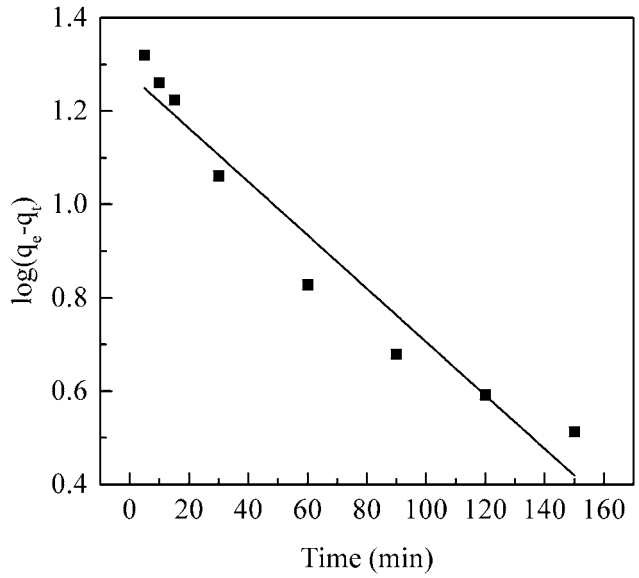

Fig. 9. Pseudo first-order kinetic plots for the adsorption of MB at 303 K.

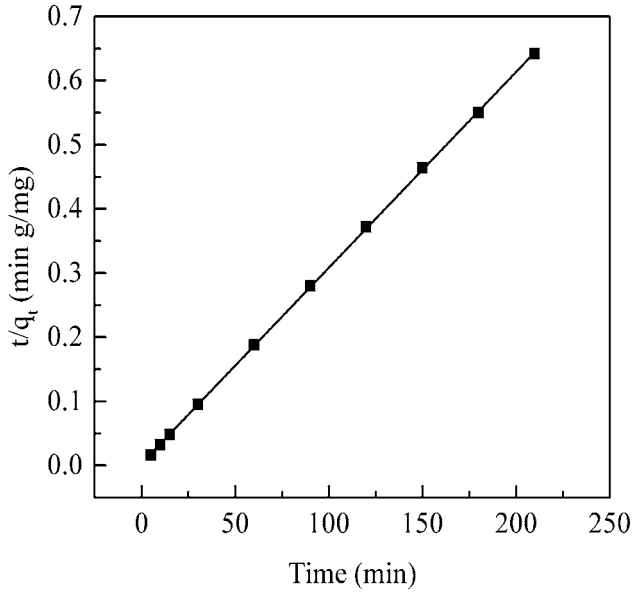

Fig. 10. Pseudo second-order kinetic plots for the adsorption of MB at 303 K.

Table 6
Kinetic parameters for the removal of MB by SA(1/50)S/500/150 at 303 K

$q_{e,exp}$ (mg/g)	Pseudo first-order model			Pseudo second-order model		
	K_1 (min^{-1})	$q_{e,cal}$ (mg/g)	R^2	K_2 (min^{-1})	$q_{e,cal}$ (mg/g)	R^2
327.1	0.0131	18.95	0.949	0.0031	333.3	0.999

4. Conclusion

The combination of sulfuric acid pretreatment and thermal regeneration is more conducive to restoring the adsorption performance of SPAC than single thermal regeneration. The regeneration effect of SPAC is strongly dependent on the conditions of regeneration. At a regeneration temperature of 500°C, a sulfuric acid concentration of 1 mol/L, a solid–liquid ratio of SPAC to sulfuric acid of 50 g/L, and a regeneration time of 150 min, SPAC achieved the best regeneration effect. The iodine value and specific surface area (iodine value of 1,037 mg/g and BET surface area of 1,314 m^2/g) of the samples obtained under the optimal regeneration conditions were higher than for virgin PAC (iodine value of 872 mg/g and BET surface area of 1,013 m^2/g). In addition, the Langmuir adsorption isotherm model showed a better correlation for the adsorption of MB on SA(1/50)S/500/150. Kinetic experiments revealed that the mechanism of MB adsorption on SA(1/50)S/500/150 followed a pseudo second-order model.

Funding

Financial support for this work from National Natural Science Foundation of China (21962001), Ningxia Scientific and Technological Innovation Leading Personnel Training (KJT2017006), Ningxia low-grade resource high value utilization and environmental chemical integration technology innovation team project are gratefully acknowledged, New Catalytic Process in Clean Energy Production (ZDZX201803).

References

[1] S. Liu, S. Jian, Z. Huang, Carbon spheres/activated carbon composite materials with high Cr(VI) adsorption capacity prepared by a hydrothermal method, J. Hazard. Mater., 173 (2010) 377–383.
[2] K. Labus, S. Gryglewicz, J. Machnikowski, Granular KOH-activated carbons from coal-based cokes and their CO_2 adsorption capacity, Fuel, 118 (2014) 9–15.
[3] X. He, Y. Geng, J. Qiu, M. Zheng, S. Long, X. Zhang, Effect of activation time on the properties of activated carbons prepared by microwave-assisted activation for electric double layer capacitors, Carbon, 48 (2010) 1662–1669.
[4] Z. Qiang, W. Ling, F. Tian, Kinetics and mechanism for omethoate degradation by catalytic ozonation with Fe(III)-loaded activated carbon in water, Chemosphere, 90 (2013) 1966–1972.
[5] Q. Li, Y. Qi, C. Gao, Chemical regeneration of spent powdered activated carbon used in decolorization of sodium salicylate for the pharmaceutical industry, J. Cleaner Prod., 86 (2015) 424–431.
[6] S.M. Nasehi, S. Ansari, M. Sarshar, Removal of dark colored compounds from date syrup using activated carbon: a kinetic study. J. Food Eng., 111 (2012) 490–495.
[7] Y.L. Yeh, A. Thomas, Color removal from dye wastewaters by adsorption using powdered activated carbon: mass transfer studies, J. Chem. Technol. Biotechnol., 63 (2010) 48–54.
[8] S. Roman, B. Ledesma, J.F. Gonzalez, A. Al-Kassir, G. Engo, A. Alvarez-Murillo, Two stage thermal regeneration of exhausted

activated carbons. Steam gasification of effluents, J. Anal. Appl. Pyrol., 103 (2013) 201–206.
[9] S.G. Huling, E. Kan, C. Caldwell, S. Park, Fenton-driven chemical regeneration of MTBE-spent granular activated carbon - a pilot study, J. Hazard. Mater., 205 (2012) 55–62.
[10] C.H. Weng, Y.T. Lin, S.C. Hsu, Electrochemical regeneration of Zn-saturated granular activated carbon from electroplating wastewater plant, Sep. Sci. Technol., 49 (2014) 506–512.
[11] E. Yagmur, S. Turkoglu, A. Banford, Z. Aktas, The relative performance of microwave regenerated activated carbons on the removal of phenolic pollutants, J. Cleaner Prod., 149 (2017) 1109–1117.
[12] K. Nath, M.S. Bhakhar, Microbial regeneration of spent activated carbon dispersed with organic contaminants: mechanism, efficiency, and kinetic models, Environ. Sci. Pollut. Res., 18 (2011) 534–546.
[13] E.T. Kostas, D. Beneroso, J.P. Robinson, The application of microwave heating in bioenergy: a review on the microwave pre-treatment and upgrading technologies for biomass, Renew. Sustain. Energy Rev., 77 (2017) 12–27.
[14] K. C Oliver, Controlled microwave heating in modern organic synthesis. Cheminform, 43 (2010) 6250–6284.
[15] E.J. Bain, J.M. Calo, R. Spitz-Steinberg, J. Kirchner, J. Axén, Electrosorption/electrodesorption of arsenic on a granular activated carbon in the presence of other heavy metals, Energy Fuels, 24 (2010) 3415.
[16] R.V. Mcquillan, G.W. Stevens, K.A. Mumford, The electrochemical regeneration of granular activated carbons: a review, J. Hazard. Mater., 355 (2018) 34–49.
[17] C.H. Weng, M.C. Hsu, Regeneration of granular activated carbon by an electrochemical process, Sep. Purif. Technol., 64 (2008) 227–236.
[18] Ö. Aktaş, F. Çeçen, Bioregeneration of activated carbon: a review, Int. Biodeterior. Biodegrad., 59 (2007) 257–272.
[19] F. Salvador, N. Martin-Sanchez, R. Sanchez-Hernandez, M. Jesus Sanchez-Montero, C. Izquierdo, Regeneration of carbonaceous adsorbents. Part I: Thermal regeneration, Microporous Mesoporous Mater., 202 (2015) 259–276.
[20] R. Pełech, E. Milchert, A. Wróblewska, Desorption of chloroorganic compounds from a bed of activated carbon, J. Colloid Interface Sci., 285 (2005) 518–524.
[21] R. Berenguer, J.P. Marco-Lozar, C. Quijada, D. Cazorlaamorós, E. Morallón, Comparison among chemical, thermal, and electrochemical regeneration of phenol-saturated activated carbon, Energy Fuels, 24 (2010) 3366–3372.
[22] I.K. Shah, P. Pre, B.J. Alappat, Effect of thermal regeneration of spent activated carbon on volatile organic compound adsorption performances, J. Taiwan Inst. Chem. Eng., 45 (2014) 1733–1738.
[23] J. Carratalá-Abril, M.A. Lillo-Ródenas, A. Linares-Solano, D. Cazorla-Amorós, Regeneration of activated carbons saturated with benzene or toluene using an oxygen-containing atmosphere, Chem. Eng. Sci., 65 (2010) 2190–2198.
[24] G.D.O. Okwadha, J. Li, B. Ramme, D. Kollakowsky, D. Michaud, Thermal removal of mercury in spent powdered activated carbon from TOXECON process, J. Environ. Eng., 135 (2009) 1032–1040.
[25] S. Román, B. Ledesma, A. Álvarez-Murillo, J.F. González, Comparative study on the thermal reactivation of spent adsorbents. Fuel Process. Technol., 116 (2013) 358–365.
[26] S.W. Nahm, G.S. Wang, PARK, YoungKwon, C.K. Sang, Thermal and chemical regeneration of spent activated carbon and its adsorption property for toluene, Chem. Eng. J., 210 (2012) 500–509.
[27] L.P. Bsc, D.E. Bsc, P.G. Bsc, K.K. Bsc, S.L. Bsc, C.S. Bsc, L. Perry, D. Essex, P. Giess, Improving the performance of granular activated carbon (GAC) via pre-regeneration acid treatment, Water Environ. J., 19 (2010) 159–166.
[28] E. Zhou, Y. He, X. Ma, G. Liu, Y. Huang, C. Chen, W. Wang, Study of the combination of sulfuric acid treatment and thermal regeneration of spent powdered activated carbons from decolourization process in glucosamine production, Chem. Eng. Process., 121 (2017) 224–231.
[29] W. He, G. Lu, J. Cu, L. Wu, L. Liao, Regeneration of spent activated carbon by yeast and chemical method, Chinese J. Chem. Eng., 20 (2012) 659–664.
[30] J. Guo, W.S. Xu, Y.L. Chen, A.C. Lua, Adsorption of NH3 onto activated carbon prepared from palm shells impregnated with H_2SO_4, J. Colloid Interface Sci., 281 (2005) 285–290.
[31] S. Brunauer, P.H. Emmett, E. Teller, Adsorption of gases in multimolecular layers, J. Am. Chem. Soc., 60 (1938) 309–319.
[32] B.C. Lippens, J.H. De Boer, Studies on pore systems in catalysts: V. The t method, J. Catal., 4 (1965) 319–323.
[33] K. Kaneko, Determination of pore size and pore size distribution: 1. Adsorbents and catalysts, J. Membr. Sci., 96 (1994) 59–89.
[34] C.O. Ania, J.B. Parra, C. Pevida, A. Arenillas, F. Rubiera, J.J. Pis, Pyrolysis of activated carbons exhausted with organic compounds. J. Anal. Appl. Pyrol., 74 (2005) 518–524.
[35] B. Ledesma, S. Roman, A. Alvarezmurillo, E. Sabio, J.F. Gonzalez, Cyclic adsorption/thermal regeneration of activated carbons. J. Anal. Appl. Pyrol., 106 (2014) 112–117.
[36] T. Karanfil, Role of granular activated carbon surface chemistry on the adsorption of organic compounds. 1. Priority pollutants. Environ. Sci. Technol., 33 (1999) 3217–3224.
[37] L. Li, P.A. Quinlivan, D.R.U. Knappe, Effects of activated carbon surface chemistry and pore structure on the adsorption of organic contaminants from aqueous solution, Carbon, 40 (2002) 2085–2100.
[38] F. Kaouah, S. Boumaza, T. Berrama, M. Trari, Z. Bendjama, Preparation and characterization of activated carbon from wild olive cores (oleaster) by H_3PO_4 for the removal of Basic Red 4, J. Cleaner Prod., 54 (2013) 296–306.
[39] M. Molinasabio, F. Rodriguezreinoso, Role of chemical activation in the development of carbon porosity, Colloids Surf., A, 241 (2004) 15–25.
[40] H.Y. Chang, H.P. Yun, R.P. Chong, Effects of pre-carbonization on porosity development of activated carbons from rice straw, Carbon, 39 (2001) 559–567.
[41] A.L. Cazetta, O.P. Junior, A.M.M. Vargas, A.P.D. Silva, X. Zou, T. Asefa, V.C. Almeida, Thermal regeneration study of high surface area activated carbon obtained from coconut shell: Characterization and application of response surface methodology, J. Anal. Appl. Pyrol., 101 (2013) 53–60.
[42] A. Sadezky, H. Muckenhuber, H. Grothe, R. Niessner, U. Poschl, Raman microspectroscopy of soot and related carbonaceous materials: spectral analysis and structural information, Carbon, 43 (2005) 1731–1742.
[43] W. Zhu, K. Arao, M. Nakamura, Y. Takagawa, K. Miura, J. Kobata, E. Marin, G. Pezzotti, Raman spectroscopic studies of stress-induced structure alteration in diamond-like carbon films, Diamond Related Mater., 94 (2019) 1–7.
[44] J. G. Wang, H. Liu, H. Sun, W. Hua, H. Wang, X. Liu, B. Wei, One-pot synthesis of nitrogen-doped ordered mesoporous carbon spheres for high-rate and long-cycle life supercapacitors, Carbon, 127 (2018) 85–92.
[45] S. Costa, B. Scheibe, M. Rummeli, E. Borowiak-Palen, Raman spectroscopy study on concentrated acid treated carbon nanotubes, Phys. Status Solidi B-Basic Solid State Phys., 246 (2009) 2717–2720.
[46] X. Ma, H. Yuan, M. Hu, A simple method for synthesis of ordered mesoporous carbon, Diamond Related Mater., (2019), 10.1016/j.diamond.2019.107480.